
Chapter 7

Conclusion and Future Scope

The main objective of the thesis was focused on the study the terahertz detectors based on mercury cadmium telluride through modeling and simulation studies. Chapter 1 provides a brief history of the terahertz region, its properties, and its applications. The outline of the thesis has also been presented. Chapter 2 provides a literature review on the detectors in the terahertz region. The state-of-the-art MCT material technology, its properties, and the motivation for the devices based on it were discussed. Major contributions of the work are summarized as follows:

7.1 Major Contributions

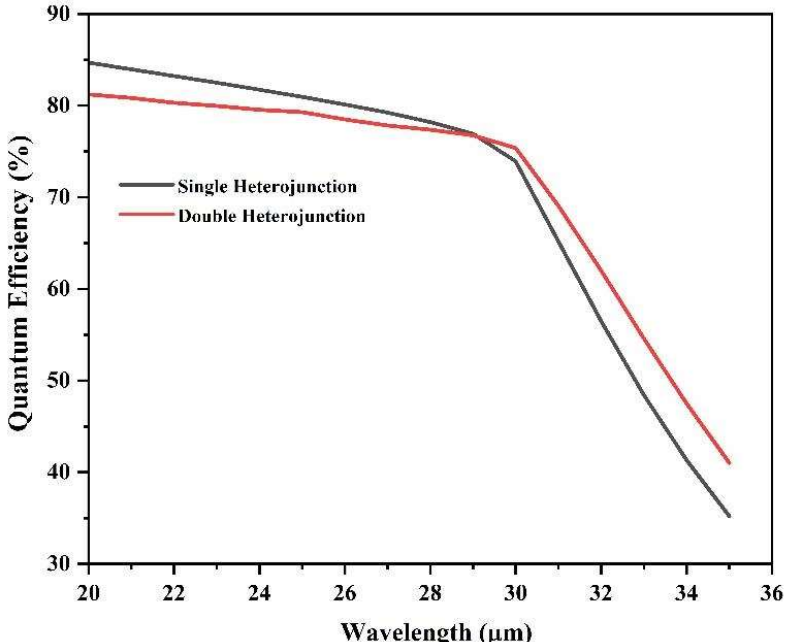
Chapter 3 studies the optoelectronic characteristics of an MCT-based single heterojunction n-i-p photodetector structure for an operating wavelength of 30 μm . CdTe material is used as a transparent window for the incident radiation to reach the MCT material. As it has very less lattice mismatch, it can able to form a good adhesive contact and a heterojunction with the MCT material absorber. The detector characteristics are summarized below.

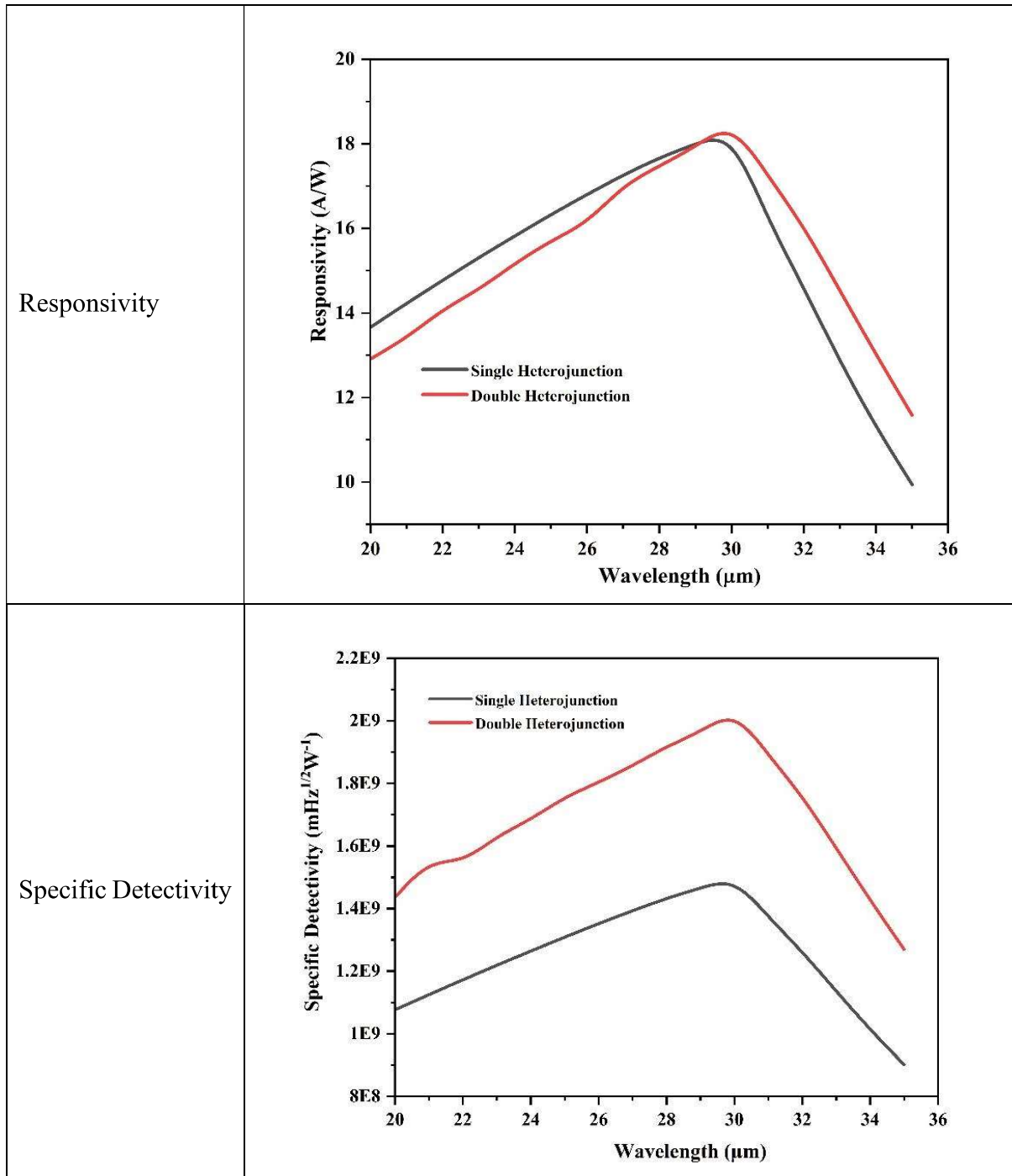
- The detector has a low dark current of $4.6 \times 10^{-9} \text{A}$.
- The quantum efficiency is found to be 73.93%.
- The responsivity is found to be 17.9 A/W.
- The detectivity is found to be $1.44 \times 10^9 \text{ mHz}^{\frac{1}{2}} \text{W}^{-1}$.
- The noise equivalent power is found to be $0.3 \times 10^{-16} \text{ WHz}^{-1/2}$.

Chapter 4 studies the optoelectronic characteristics of an MCT-based double heterojunction n-i-p photodetector structure for the THz application. The presence of a second heterojunction accounted for the reduction of diffusion current. Thus, resulting in a reduction of dark current in the device and thus exhibited enhanced optoelectronic characteristics. The device exhibited the following characteristics.

- The detector has a low dark current of $2.42 \times 10^{-10} A$.
- The quantum efficiency is found to be 75.35%.
- The responsivity is found to be 18.21 A/W.
- The detectivity is found to be $1.99 \times 10^9 mHz^{\frac{1}{2}} W^{-1}$
- The noise equivalent power is found to be $0.21 \times 10^{-16} WHz^{-1/2}$.

Table 7.1 Comparison of the proposed single and double heterojunction photodetectors

Parameter	Graphical Comparison																														
Quantum Efficiency	 <p>The graph plots Quantum Efficiency (%) on the y-axis (ranging from 30 to 90) against Wavelength (μm) on the x-axis (ranging from 20 to 36). Two data series are shown: 'Single Heterojunction' (black line) and 'Double Heterojunction' (red line). Both start at approximately 85% efficiency at 20 μm. The Single Heterojunction efficiency drops to about 75% at 30 μm and then sharply to ~35% at 35 μm. The Double Heterojunction efficiency remains above 75% at 30 μm and drops to about 40% at 35 μm, showing superior performance at longer wavelengths.</p> <table border="1" data-bbox="532 1205 1312 1843"> <caption>Approximate data points from the Quantum Efficiency graph</caption> <thead> <tr> <th>Wavelength (μm)</th> <th>Single Heterojunction (%)</th> <th>Double Heterojunction (%)</th> </tr> </thead> <tbody> <tr> <td>20</td> <td>85</td> <td>81</td> </tr> <tr> <td>22</td> <td>83</td> <td>80</td> </tr> <tr> <td>24</td> <td>81</td> <td>79</td> </tr> <tr> <td>26</td> <td>79</td> <td>78</td> </tr> <tr> <td>28</td> <td>77</td> <td>77</td> </tr> <tr> <td>30</td> <td>75</td> <td>76</td> </tr> <tr> <td>32</td> <td>55</td> <td>65</td> </tr> <tr> <td>34</td> <td>40</td> <td>50</td> </tr> <tr> <td>35</td> <td>35</td> <td>40</td> </tr> </tbody> </table>	Wavelength (μm)	Single Heterojunction (%)	Double Heterojunction (%)	20	85	81	22	83	80	24	81	79	26	79	78	28	77	77	30	75	76	32	55	65	34	40	50	35	35	40
Wavelength (μm)	Single Heterojunction (%)	Double Heterojunction (%)																													
20	85	81																													
22	83	80																													
24	81	79																													
26	79	78																													
28	77	77																													
30	75	76																													
32	55	65																													
34	40	50																													
35	35	40																													



Chapter 5 studies the optoelectronic characteristics of a graphene/n-MCT Schottky diode detector. The advantage of this structure is the thickness of the metal contact (graphene) is very less allowing most of the incident radiation to reach the active region. Another aspect is its

structural advantage forming a barrier and blocking one type of carrier unlike p-n and p-i-n detectors. Thus, the device has a less dark current.

- The detector has a low dark current of $5.4 \times 10^{-11} \text{ A}$.
- The quantum efficiency is found to be 77.88%.
- The responsivity is found to be 18.6 A/W.
- The detectivity of the device is found to be $1.41 \times 10^{11} \text{ mHz}^{\frac{1}{2}} \text{ W}^{-1}$.
- The noise equivalent power is found to be $0.71 \times 10^{-17} \text{ WHz}^{-1/2}$.

Table 7.2 Comparison of the proposed photodetectors

Parameter	Single Heterojunction	Dual Heterojunction	Schottky Diode Detector
Operating wavelength (μm)	30	30	30
Current under Dark Condition (A)	4.6×10^{-9}	2.6×10^{-10}	5.4×10^{-11}
Quantum Efficiency (%)	73.93	75.35	77.88
Responsivity (A/W)	17.9	18.21	18.6
Specific Detectivity ($\text{mHz}^{1/2} \text{ W}^{-1}$)	1.44×10^9	1.99×10^9	1.41×10^{11}
Noise Equivalent Power ($\text{WHz}^{-1/2}$)	0.3×10^{-16}	0.21×10^{-16}	0.71×10^{-17}

Chapter 6 studies a graphene-gated semiconductor THz detector. Graphene is a semi-metal and is used as a gate contact. Its thickness is so low that it allows most of the incident THz radiation to reach the semiconductor (MCT channel). Under the influence of illumination, two effects namely photoconductive and photovoltaic cause a change in the current flowing in the channel. In the proposed GSFET device, the channel current is controlled entirely by the incidence of THz radiation.

The following are the outcomes of the proposed GSFET:

- The THz detector is sensitive to power of $P_{in} = 0.88 \times 10^4 W/m^2$
- The drain current under illumination is found to be 127.07 mA.
- The drain current under dark conditions is found to be 4.52 mA.
- The device is found to have an optical gain of 27.11.
- The device is found to have a transconductance of 36.18 mA/V.

7.2 Future Scope

In the present work, sincere effort has been put into exploring the possibilities of MCT-based devices for the THz regime. Since a time-bound is present in the Ph.D. program and also during the program, Covid has put a break on the research, it was not possible to analyze the devices in all aspects. As research is a continuous process, there is always scope for further work in this area.

- ❖ nBn detectors may be designed and analyzed.
- ❖ A multicolour detector capable of detecting THz/LWIR/MWIR may be designed and analyzed.
- ❖ Along with the thermionic emission theory, drift-diffusion theory may also be useful for accurate analysis of the Schottky diode detector.
- ❖ An analysis may be carried out on an MIS detector structure that can yield better results than a simple Schottky diode detector.
- ❖ An MSM type of structure can be designed and modeled using graphene as a metal on both the sides.

- ❖ Gate voltage bias-dependent analysis may be carried out in the GSFET structure in addition to the effect of incident radiation.
- ❖ Analysis may be carried out including the effects of different recombination mechanisms.
- ❖ Analytical modeling may be carried out on the GSFET structure for MWIR and LWIR regions.

Finally, it may be pointed out that our work is purely theoretical and some supported with numerical simulations. Due to the unavailability of the THz source, experimental studies could not be carried out. In the future with the availability of the source, the theoretical studies must be validated by experimental investigations. However, the theoretical studies carried out by us will motivate the design engineers to carry out the necessary experimental studies.